

## Referenzexperiment zum Aerosolpartikel-Transport für dynamische Situationen

### Reference experiment for aerosol particle transport for dynamic situations

Sebastian Merbold<sup>1</sup>, Gazi Hasanuzzaman<sup>1</sup>, Tom Buchwald<sup>1</sup>, Christoph Schunk<sup>2</sup>, Daniel Schmeling<sup>3</sup>, André Volkmann<sup>3</sup>, Robert Brinkema<sup>3</sup>, Uwe Hampel<sup>2</sup>, Andreas Schröder<sup>1,4</sup>, Christoph Egbers<sup>1</sup>

<sup>1</sup>Brandenburgisch Technische Universität Cottbus-Senftenberg, Lehrstuhl Aerodynamik und Strömungslehre, Cottbus, Deutschland

<sup>2</sup>Helmholtz-Zentrum Dresden-Rossendorf, Institut für Fluidodynamik und Technische Universität Dresden, Professur für Bildgebende Messverfahren für die Energie- und Verfahrenstechnik

<sup>3</sup>Deutsches Zentrum für Luft- und Raumfahrt (DLR), Institut für Aerodynamik und Strömungstechnik, Bodengebunde Fahrzeuge (AS-BOA), Göttingen

<sup>4</sup>Deutsches Zentrum für Luft- und Raumfahrt (DLR), Institut für Aerodynamik und Strömungstechnik, Experimentelle Verfahren (AS-EXV), Göttingen

Aerosol, Visualisierung, PIV, PTV STB, Partikelsensoren, Raumventilation

Aerosol, visualization, PIV, PTV STB, particulate matter sensors, room ventilation

### Abstract

To study transport of aerosol particles in closed rooms we set up the Cottbus aerosol particle reference experiment (CARE) including thermal manikins and a spreader dummy. For various flow configurations (location of spreader, heating bodies, windows opened, air purification systems used) flow visualisation is performed, particulate matter sensors measure local particle concentrations, head mounted camera systems count particle concentrations of individuals and large field of view Shake-The-Box Particle Tracking delivers velocities. We here discuss the experimental configuration of simultaneous particle counting, tracking and velocity measurements inside CARE.

### Introduction

Airborne transport of aerosol particles is the main path of SARS-CoV-2, measles or other respiratory virus infections in closed rooms. Infection risks must be determined through parametric dispersion studies, which can be done by simulations and experiments. Recently, the complete flow inside a 12 m<sup>3</sup> generic test room including a thermal breathing human model was investigated successfully by using sub-millimetre sized Helium-Filled-Soap-Bubble (HFSB) tracers, pulsed LED-arrays and the STB particle tracking technique (Schröder et al. 2022). Aerosol generation and detection systems were also applied to aircraft cabins (Schmeling et al., 2022-1) and train compartments (Schmeling et al., 2022-2). The most approaches to study aerosol transport are in static situations, however, in real world, most situations are rather dynamic with e.g. people walking around, which is expected to have an impact on the aerosol distribution in the room. In preparation we set up the Cottbus aerosol particle reference experiment (CARE) and use several measurement techniques to reveal the flow fields and especially the aerosol transport and traces. Head mounted camera system is built and particulate matter

sensors are adapted in huge number inside the room, allowing a space and time resolution of the local concentration. The flow visualisation is performed for various flow configurations (location of spreader, heating bodies, windows opened, air purification systems used). Large field of view Shake-The-Box Particle Tracking deliver long time-series of several square meters sized Lagrangian and Eulerian velocities. We here discuss the experimental configuration of simultaneous particle counting, tracing and velocity measurements inside CARE.

### Cottbus aerosol particle reference experiment (CARE)

The reference room for aerosol particle transport (schematic presented in Figure 1a) is located in Cottbus at Brandenburg University of Technology. The room is divided into three principle segments, main experimental chamber, control room and measurement support chamber. All three segments are thermally insulated in order to prevent the loss of heat. The main experimental chamber (mec) has a rectangular shape with height of 2.8 m. One side of this chamber is equipped with four windows and an entrance door is located on the other side of the room. In order to conduct undisturbed measurements without any external influence, control equipment is placed in the control room. The mec adjoins the measurement support chamber, where LED light arrays are located, a transparent window is attached within the partition for the optical access from LED arrays.

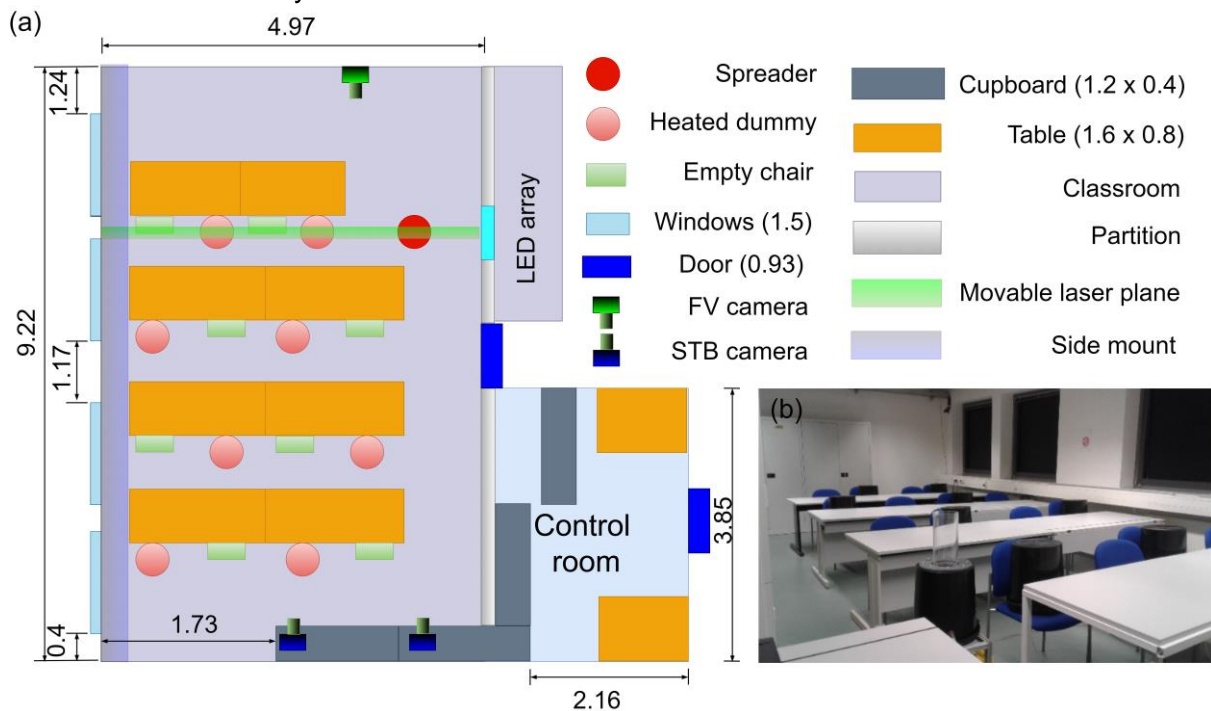


Figure 1: Schematic of the CARE in (a) and photograph in (b). All dimensions are given in meters.

A seating arrangement for 16 students is organized to replicate an ideal classroom scenario, alternating chairs are equipped with heated dummy (see Figure 1 a,b). The energy input created by students is modelled with these dummies, which consists of a black cylinder and an 80 Watts incandescent bulb. The temperature on the outer shell of the cylinder stabilizes within 40 minutes to 37°C.

For various flow situations (location of dummies and spreader, windows open, heater on, air purification systems used) the large-scale behaviour of the convective plumes and rolls are inspected by qualitative flow visualization (Figure 2). The flow visualization was done with a

continuous wave laser and Di-Ethyl-Hexyl-Sebacat (DEHS) particles with  $\sim 0.2 \mu\text{m}$  size (Hasanuzzaman et al. 2022). Figure 2 shows the flow visualization images where heating the dummies creates significant changes in the room flow, up and down washing due to convection is indicated by the yellow and blue arrows respectively.

For extensive studies of aerosol particle transport inside CARE different measurement techniques are applied, leading to different requirements for the seeding particles. The DEHS particles are suited for the general aspect of aerosol transport as they can be seeded very easily and cost efficient while artificial saliva droplets are used for measurements using multiple aerosol particulate matter sensors. Both are representing the size distribution of aerosol particles exhaled by humans. To follow particle tracks by STB or to count them in the head mounted systems larger particles are needed, where we use HFSB. By means of all three seeding techniques, we can analyse all essential features of the aerosol transport inside rooms.

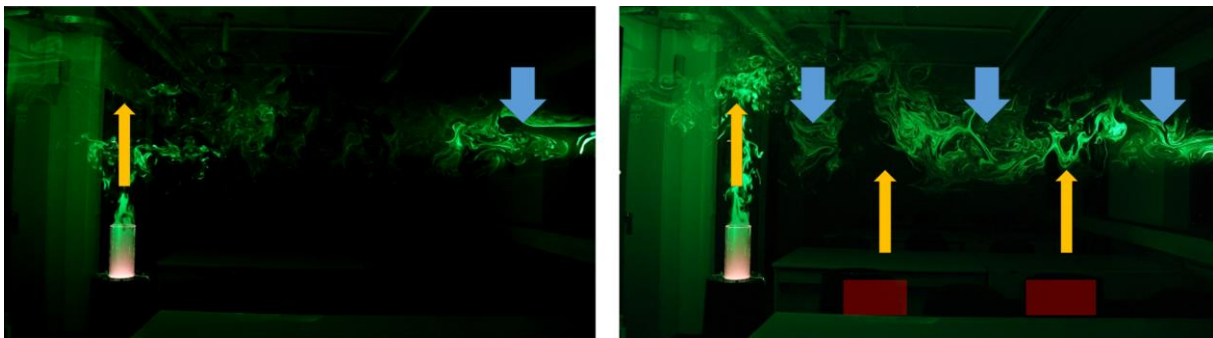


Figure 2: Flow visualization photographs without dummies heating (left) and with heating (right). Here, heated dummies are presented with red boxes, orange and blue arrows indicate the mean movement of the convective plumes and rolls.

### Head mounted camera systems

We developed an inexpensive head mounted camera system to detect HFSB with a diameter of approximately  $350 \mu\text{m}$ . These buoyancy neutral particles are detected and counted with an integrated particle detection algorithm. The head mounted part consists of a Dräger full face mask and a 3D printed inlet, instead of the usual gas filter (Figure 3 left). The inlet has a diameter of 11 cm and is covered with a combined FFP2, black Molton fleece. A tripod with a camera is attached above the inlet (Figure 3 center). It faces perpendicular to the inhalation hole and is connected via an elongated ribbon cable to a Raspberry Pi single board computer. The measuring area is illuminated with a ring light, which creates a light curtain that is about 1.5 cm thick. The HFSB that pass this area are detected by the camera (Figure 3 right). The whole system (Raspberry Pi and LED ring light) is powered by a standard power bank in a small bag that is worn on the body. To supply the ring light with the needed voltage, a step-up converter is used to convert the 5 volts to the needed 12 volts for the LEDs. We also provide a charging station to easily recharge multiple power banks at once.

All computers are accessible via a local Wi-Fi network using a high-speed WLAN router. Each single board computer is assigned to an individual static IP address and can be controlled via a simple web-based user interface, which offers a live web stream of the camera view. The web frontend allows the user to control basic settings like resolution, contrast, brightness, ISO and shutter speeds. Furthermore, the experimenter can set the calibration values for the horizontal and vertical pixel resolution and define a detection passe-partout within the camera view. Various commands like capturing still images, videos, image sequences or starting the

integrated object detection can be triggered. Because all commands are simple HTTP requests, the cameras can also be remote-controlled by a script without the use of a graphical user interface. The recordings are stored on the device itself and can be downloaded from the provided web interface. In addition to the standard user interface, a master camera administration application is provided. Most of the options which are available to control a single camera are also available in a broadcast variant in this application. Commands like the image capturing functionality can be triggered for all cameras with a single request. The web-based software and the camera control logic was written in Python and is running on a stripped-down Raspberry Pi Linux operating system. When the system is switched on, the camera application starts automatically as a system service. In case of an error, this service will be automatically restarted.



Figure 3: Left: Dräger mask with power bank and single board computer. Center: Inlet with camera mounted on a tripod. Right: Helium-filled soap bubbles (HFSB) captured with the head mounted camera system (enlarged).

### Multiple aerosol particulate matter sensors

For the time and space resolved analysis of the spreading of aerosol particles in the test room, an additional measurement system based on a source of artificial saliva aerosol particles and multiple aerosol particulate matter sensors is applied. The source is based on an atomization system, a reservoir of artificial saliva (according to NRF7.5) and well-defined volume flow rates. This generator is connected via a pipe to a facial mask. For the detection, more than 30 particulate matter sensors are distributed in the room. Details can be found in Schiepel et al. (2021). The data acquisition is accomplished by a mobile measurement system (see Niehaus (2022) and Niehaus and Westhoff (2022)). The aerosol generation and detection system were also applied to aircraft cabins (Schmelting et al., 2022-1) and train compartments (Schmelting et al., 2022-2). The measurement layout of the particle sizer measurements is depicted in Figure 4.

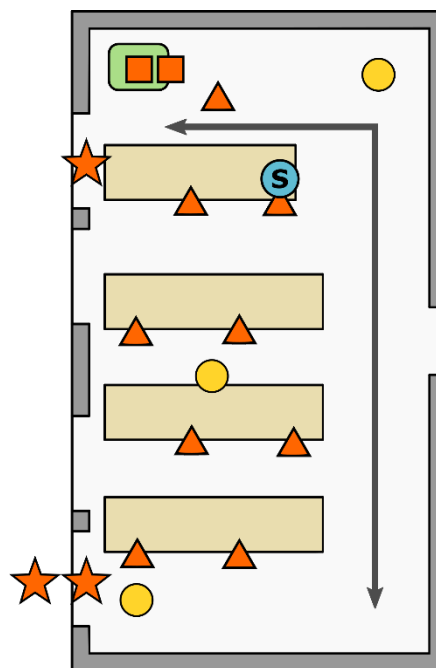


Figure 4: Measurement configuration inside CARE. Sensor positions: triangle: on 1.1 m height, circle: four sensors on different heights, star: in window area (inside and outside), square: suction and exhaust of air purifier. The arrow reflects the pathway of the movement. Windows are located on the left side of the room. The source is located on the front desk at the right end.

Figure 5 shows the time-resolved local aerosol concentration measured on the rear right seat next to the aisle for four different cases: no-ventilation (=baseline), an interval window opening, an interval window opening with additional movement in the room, and an air purifier running on 600 m<sup>3</sup>/h. For the case with no ventilation (purple), the aerosol concentration significantly starts to increase after about 900 s after starting the emission of aerosol particles. Until this point in time, the aerosol particles did not reach the sensor position. After this instant in time, the concentration increases rather monotonic reaching values up to 1200 particles per cm<sup>3</sup> towards the end of the measurement run. In contrast, the case with air purifier and movement (green) reveals much earlier increase of the local concentration, even before the person starts moving (black dashed line). The additional air flow in the room, induced by the air purifier, leads to a faster transport of the particles to the rear of the room. However, with the start of the movement, stationary aerosol concentration around 350-400 particles per cm<sup>3</sup> are found. Here the additional mixing in the room in combination with the cleaning capability of the air purifier balances the aerosol production rate of the source. The two window opening cases without (blue) and with (red) movement reveal similar concentration developments, both showing strong decreases of the concentration during window opening (light green areas). During this five minutes window opening period the local concentration falls by around 700 particles per cm<sup>3</sup>. However, the additional movement in the room induces an additional air mixing in the room, which transports the aerosol particles faster to the rear (compare blue and red curve in time interval 600 s – 1200 s).

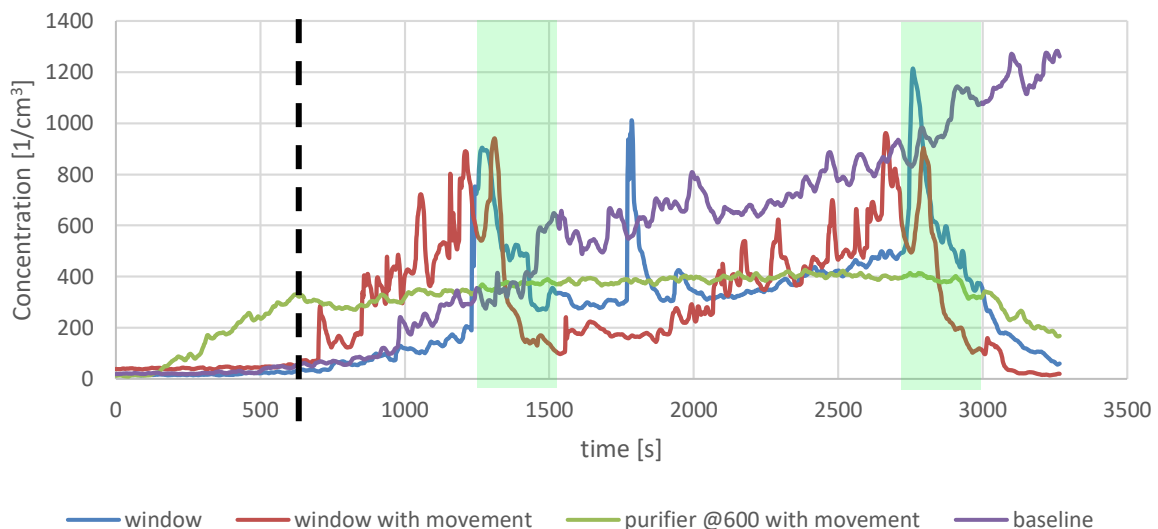
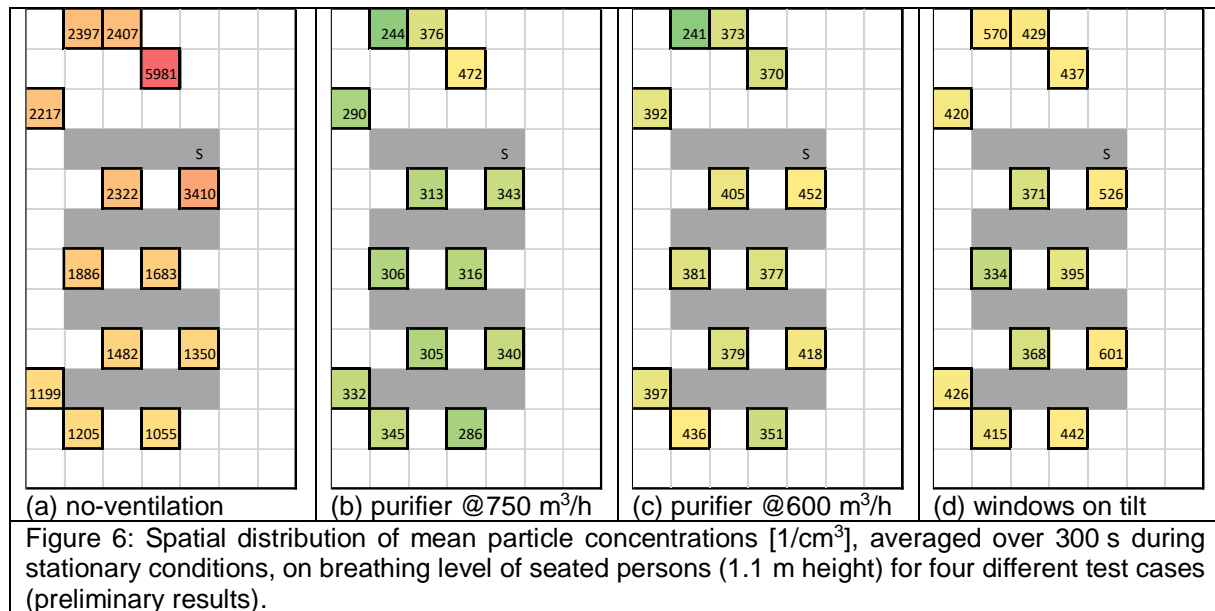


Figure 5: Local aerosol concentration [1/cm<sup>3</sup>] on rear right seat at aisle at 1.1 m height for no-ventilation case, with air purifier and with interval window opening. Light green background highlights periods of window opening. Vertical dashed line marks start of movement (preliminary results).

Figure 6 presents the time averaged aerosol concentration for selected sensor positions and cases. Here only cases are shown, where stationary aerosol concentrations were reached, i.e., no interval window opening (except the no-ventilation case). In Figure 6(a) the no-ventilation case reveals very high concentrations which decrease with increasing distance from the source (S). All other presented cases show much lower values and more homogeneous distributions in the room. Here the case with the purifier on 750 m<sup>3</sup>/h (Figure 6(b)) shines out with

lowest values. The case with the tilted windows (Figure 6(d)) reflects lowest values in the centre of the room close to the windows (left side), which increase in front, rear and side of the room.

The briefly presented results in this section highlight two main points; firstly, the value of these fast, cost-efficient and easy to install measurement technique providing spatial and temporal resolution. Secondly, they show the clear effect of the different ventilation cases on both, the spatial aerosol distribution and the time-development of the aerosol particle concentration.



## Large field of view Shake-the-Box Particle Tracking

In addition to the aerosol concentration measurements, experiments were conducted to investigate the mixed convective flow in a large-scale planar sub-volume with  $\sim 40$  cm thickness in the front area of the model classroom using a 2D-LPT-tracking approach based on the volumetric Shake-The-Box (STB) algorithm (Schanz et al. 2016). Similar to Schröder et al. 2022, a corresponding 2D LPT set-up is employed, while the reference case without moving people, open windows or running room air purifier is considered. Two pulsed linear LED arrays with 2.8 m length and collimating lenses were installed opposite to a mirror array to provide a wide light sheet illuminating a plane of 5 m x 2.8 m in the front row of seats (Figure 1). Two Bonito-PRO X-2620B cameras with a pixel size of  $4.5 \mu\text{m}$  and a resolution of 5120 x 5120 pixels equipped with  $f=50$  mm Nikon lenses in the back of the room were used to acquire particle images with a greylevel depth of 10 bits. The German Aerospace Center (DLR) in Göttingen provided both LED arrays and cameras. Image acquisition and LED illumination were triggered synchronously with 45 Hz in order to resolve the Lagrangian particle tracks in regions of higher velocities. These appear especially in the thermal plumes created by the heated dummies, in vicinity to the air purifier or with opened windows. Due to the large volume, only particles that reflect a sufficient amount of light can be considered as seeding material. HFSB meet this requirement due to their mean size of  $\sim 350 \mu\text{m}$  and their favorable reflection properties. To fill the room with neutrally buoyant particles a HFSB generator from LaVision with 130 nozzles was used. Due to the large number of nozzles, a sufficient particle density could be achieved despite the large illuminated volume and the limited lifetime of the HFSB. To exclude influence of the momentum of HFSB generation onto the flow situation, image acquisition was started two minutes after seeding.

First, a camera calibration and the estimation of the particles Optical Transfer Function (OTF) for each camera and sub-plane has been processed (Schanz et al. 2013). The process determines the parameters of the average shape of particle images in dependence of the position on the camera sensor. Then the STB algorithm (Schanz et al. 2016) has been applied to the series of time-resolved particle images from the two cameras. A two-pass 2D-STB approach was employed, which first tracks forward in time, then reverses the image order and elongates existing tracks backward in time, while reconnecting possible track-fragments. The special feature of the STB algorithm is not only the prediction of the particle's positions in the next time step by extrapolation of already existing tracks, but as well the corresponding correction of this predicted position by using the previously determined OTFs and a local steepest gradient method ('shaking'-approach). Each particle position is then adjusted via an iterative process (shaking), so that the intensity of the residual image is minimized. The resulting particle tracks are stored after a temporal filter using third order B-splines with optimal weighting coefficients is applied.

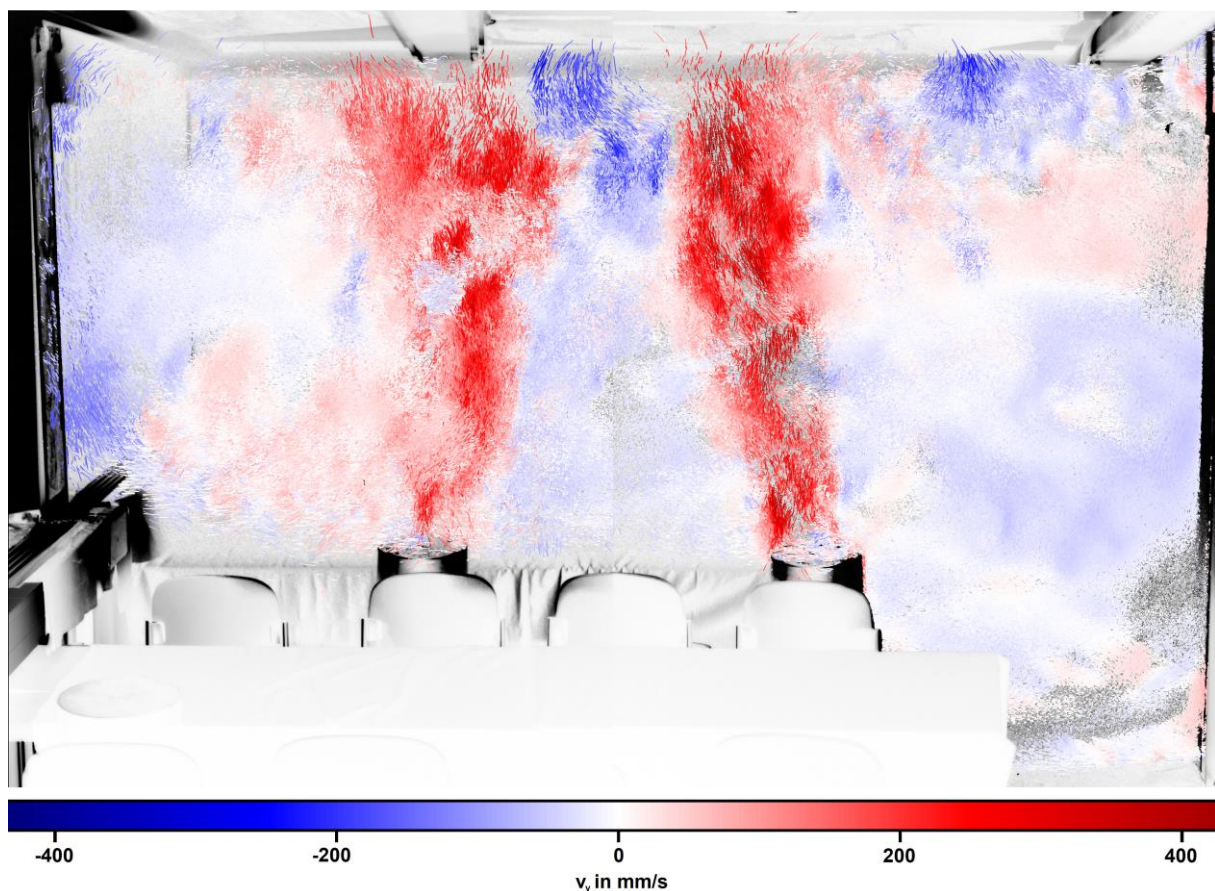


Figure 7: Lagrangian particle tracks of the reference case with no windows open, room air cleaner turned off, and no people moving. The tracks in the foreground are color coded with the vertical velocity component, while a negative of the classroom can be seen in the background (preliminary results).

Figure 7 contains the Lagrangian particle tracks from both (partly overlapping) camera perspectives. Since the wide light section of about  $\sim 40$  cm thickness shows particle tracks one behind the other, the three-dimensional nature of the flow can be observed. Using long time-series of particle images and corresponding Lagrangian particle tracks a bin-averaging procedure allows to create mean and Reynolds stress statistics. On the other hand, transient pro-

cesses of dynamic conditions and their effect on the particles transport properties and respective flow structures can be investigated. Results of the dynamic conditions will be presented on the conference.

## Conclusion

A reference room for aerosol particle transport was established at BTU Cottbus-Senftenberg (CARE), where various classroom situations are analysed using seated thermal manikins, inducing turbulent thermal plumes and mixed convection flows inside the test room. We use several measurement techniques to reveal the flow fields and especially the aerosol transport and traces. Flow visualisation is performed for analysis of various flow configurations (location of spreader, heating bodies, windows opened, air purification systems used). STB will deliver long time-series of several m<sup>2</sup> sized Lagrangian and Eulerian velocity fields. We here discuss the experimental configuration of simultaneous particle counting, tracing and velocity measurements inside CARE. In a further study, the dynamic situations involving several moving persons in combination with the above described measurement techniques we will evaluate the amount of potentially inhaled aerosol particles at the individuals.

## Acknowledgement

We acknowledge the financial support by the Deutsche Forschungsgemeinschaft under grant number DFG EG100/36-1, HA3088/25-1 and SCHR1165/6-1. Work of BTU-CS was partially supported by BTU Graduate Research School (CTG).

Work of DLR-AS-BOA was partially supported by the Initiative and Networking Fund of the Helmholtz Association of German Research Centres (HGF) under the CORAERO project (KA1-Co-06).

## References

- Hasanuzzaman, G., Merbold, S., Motuz, V. and Egbers, Ch. 2022:** Enhanced outer peaks in turbulent boundary layer using uniform blowing at moderate Reynolds number, *Jour. Turb.*, DOI: 10.1080/14685248.2021.2014058, pp. 1 - 29.
- Shih, W.C.L., Wang, C., Coles, D., Roshko, A., 1993:** Experiments on flow past rough circular cylinders at large Reynolds numbers. *J.Wind Eng. Ind. Aerodyn.* 49:351–368
- Niehaus, K., Westhoff, A., 2022:** “An Open-Source Data Acquisition System for Laboratory and Industrial Scale Applications” *Measurement Science and Technology* (submitted)
- Schmeling, D., Shishkin, A., Schiepel, D., Wagner, C., 2022-1:** “Numerical and experimental study of aerosol dispersion in the Do728 aircraft cabin” *CEAS Aeronautical Journal* (submitted)
- Schmeling, D., Kühn, M., Schiepel, D., Dannhauer, A., Lange, P., Kohl, A., Niehaus, K., Berlitz, T., Jäckle, M., Kwitschinski, T., Tielkes, T., 2022-2:** “Analysis of Aerosol Spreading in a German Inter City Express (ICE) Train Carriage”, *Building and Environment* (under review)
- Schiepel, D., Niehaus, K., Schmeling, D., 2021:** “Generation, Detection and Analysis of Aerosol Spreading Using Low-Cost Sensors” In: *Proceeding of the European Aerosol Conference*
- Niehaus, K., 2022:** “Mobile measurement system” <https://doi.org/10.5281/zenodo.6471388>
- Schanz, D., Gesemann, S., Schröder, A. 2016:** Shake The Box: Lagrangian particle tracking at high particle image densities, *Exp. Fluids* 57:70
- Schanz, D., Gesemann, S., Schröder, A., Wieneke, B., Novara, M., 2013:** Non-uniform optical transfer function in particle imaging: calibration and application to tomographic reconstruction, *Meas Sci Technol* 24, 024009
- Gesemann, S., Huhn, F., Schanz, D., Schröder, A., 2016:** From Noisy Particle Tracks to Velocity, Acceleration and Pressure Fields using B-splines and Penalties, 18th Lisbon Symposium, Portugal using PIV and 2D- and 3D- Shake-The-Box
- Schröder A, Schanz D, Bosbach J, Novara M, Geisler R, Agocs J, Kohl A. 2022.** Large-scale volumetric flow studies on transport of aerosol particles using a breathing human model with and without face protections, *Physics Fluids* 34, 035133.